J. Applied Membrane Science & Technology, Vol. 30, August 2026, 136-150

Development of Biodegradable Thermoplastic Potato Starch Formulations for Sustainable HVAC Air Filter Frames

Z. Y. Wong[1], K. C. Chong[1,2*], H. K. Kam[1,2], S. O. Lai[1,2], Fang Wang[1,3], W. C. Chong[1,2], W. C. Cheong[1,2]

[1]Lee Kong Chian Faculty of Engineering and Science, Universiti Tunku Abdul Rahman (UTAR), Jalan Sungai Long, Kajang 43000, Selangor, Malaysia
[2]Centre for Advanced and Sustainable Materials Research, Universiti Tunku Abdul Rahman, Jalan Sungai Long, Kajang 43000, Selangor, Malaysia
[3]College of Chemistry and Chemical Engineering, Dezhou University, Dezhou 253023, China

Submitted: 08/06/2026. Revised edition: 26/06/2026. Accepted: 27/06/2026. Available online: 21/08/2026

ABSTRACT

The HVAC sector relies heavily on petroleum-based engineering plastics, particularly for rigid HEPA filter frames. Because these frames are permanently bonded to filter media, spent assemblies generate a massive landfill waste stream. This study investigates a sustainable alternative utilizing potato starch (*Solanum tuberosum*) plasticized with glycerol via hydrothermal gelatinization. The formulation systematically varied the plasticizer-to-starch weight ratio (0% to 100%) to optimize mechanical and environmental performance. Mechanical testing revealed an inverse relationship between plasticizer loading and ultimate tensile stress. The optimized formulation (25% wt. glycerol) achieved a maximum tensile strength of 2.940 MPa, balancing structural integrity with flexibility, while higher loadings drastically reduced capacity due to molecular lubrication. FTIR spectroscopy confirmed successful matrix plasticization and preservation of the primary polysaccharide backbone. Six-week terrestrial soil burial assays demonstrated continuous microbial and hydrolytic degradation across all thermoplastic starch formulations. The optimized matrix exhibited the fastest biodegradation kinetics, reaching a cumulative gravimetric mass loss of 79.09% by week six due to enhanced hydrophilicity and microbial accessibility. These findings demonstrate that plasticizer optimization can precisely tailor biopolymer properties, positioning potato starch-based frameworks as viable, eco-friendly candidates for disposable HVAC components and sustainable packaging.

Keywords: Thermoplastic starch (TPS); Potato starch; Glycerol plasticization; Biodegradable filter frames; HVAC sustainability; Soil burial degradation

1.0 INTRODUCTION

Anthropogenic plastic pollution has precipitated a global ecological crisis, prompting stringent regulatory mandates that restrict petroleum-based polymers and incentivize biodegradable alternatives. While this green transition has gained significant commercial

* Corresponding to: K. C. Chong (email: chongkc@utar.edu.my)
DOI: https://doi.org/10.11113/jamst.v30n2.349

traction in flexible packaging and single-use consumer items, the Heating, Ventilation, and Air Conditioning (HVAC) sector remains heavily reliant on non-biodegradable synthetics. Within modern building infrastructure, commercial and residential air filtration units are critical for removing airborne contaminants, capturing fine particulate matter, and maintaining healthy Indoor Air Quality (IAQ) [1].

However, the structural framing of these filters represents an unaddressed and highly problematic waste stream. To minimize fabrication costs and ensure high dimensional stability, manufacturers typically fabricate frames from rigid, petroleum-based injection-molded plastics. Specifically, conventional filter frames rely on fossil-fuel-derived polymers such as high-impact polystyrene (PS), polypropylene (PP), or acrylonitrile butadiene styrene (ABS) [2]. These engineering plastics are selected because they exhibit high flexural rigidity, excellent tensile capacity, and moisture resistance. Such properties are vital to ensure the structural frame can securely support the filter media and successfully withstand severe operational pressure drops (ΔP) under continuous, high-velocity airflow fields without buckling, warping, or causing bypass leakage around the tracking seals.

Despite their structural utility, these synthetic frames impose a severe ecological burden at their end-of-life. High-Efficiency Particulate Air (HEPA) filters require complete replacement every 6 to 12 months due to progressive particulate loading, which restricts airflow and reduces system efficiency [3]. Because these non-biodegradable plastic frames are permanently bonded to the delicate fiberglass or synthetic filter media using heavy polyurethane adhesives to guarantee an airtight seal, spent assemblies cannot be economically separated or recycled.

Consequently, hundreds of millions of these bulky, multi-material air filter units are discarded annually across the globe. This baseline operational turnover translates directly into thousands of tons of compounded, unrecyclable plastic waste that is routed to municipal landfills or incineration facilities every year, where it either persists indefinitely or releases toxic greenhouse gas emissions [4]. In municipal landfill ecosystems, these rigid frames resist natural degradation pathways for centuries. Therefore, there is a critical need for eco-friendly structural materials capable of replacing conventional engineering plastics without compromising HVAC component integrity [5]. Crucially, while primary load-bearing automotive or aerospace components demand extreme mechanical properties, disposable HVAC frames operate under static, low-load conditions within fixed structural tracking channels. This specific low-demand structural profile means they can be successfully substituted by specialized bio-based polymer frames, offering a highly sustainable material pathway where complex dynamic loading requirements are minimal.

To mitigate the end-of-life limitations of conventional frames, natural bio-based polymers offer a viable pathway toward circular design. Starch-based polymers comprising linear amylose and branched amylopectin chains present unique advantages due to their rapid biodegradation kinetics, low carbon footprint, and ubiquitous availability from agrarian feedstocks (*Zea mays, Solanum tuberosum,* and *Manihot esculenta*) [6, 7]. In its native state, neat starch exhibits severe performance limitations, including high brittleness, poor processability, and low tensile strength caused by strong intermolecular hydrogen bonding between its tightly packed hydroxyl networks. To convert native starch granules into processable

* Corresponding to: K. C. Chong (email: chongkc@utar.edu.my)
DOI: https://doi.org/10.11113/jamst.v30n2.349

Thermoplastic Starch (TPS), the dense crystalline structure must be systematically destructurized. This is achieved by introducing low-molecular-weight plasticizers and additives (e.g., glycerol, urea, dilute hydrochloric acid, or sodium bicarbonate) under specific thermal, hydrothermal, and mechanical shear fields [8, 9]. These agents disrupt the native crystalline domains and substitute starch-starch hydrogen bonds with highly stable starch-plasticizer interactions, significantly enhancing the free volume, molecular chain mobility, ductility, and flexural modulus of the resulting polymer matrix [10]. This molecular rearrangement transforms the rigid granular carbohydrate into a workable, form-stable melt that can be cast or injection-molded into functional component shapes.

In this study, potato starch (*Solanum tuberosum*) was selected as the primary biopolymer precursor. Compared to conventional cereal starches like corn or wheat, potato starch features larger native granule sizes (up to 100 μm), a relatively high amylose content (~20–25%), a lower gelatinization temperature, and a unique presence of covalently bound phosphate ester groups on the amylopectin structure [11]. These characteristics yield superior film-forming capabilities, excellent matrix consistency, and enhanced mechanical properties post-plasticization, rendering it a highly promising candidate for biodegradable, structurally stable HVAC filter frames.

While the fundamental material chemistry of starch/glycerol thermoplastic systems is well established in literature for flexible packaging films, the application of targeted biopolymer design to replace rigid engineering plastics in localized building infrastructure remains unexplored. Therefore, the primary novelty of this study lies in the targeted engineering and practical application of optimized, tailored potato-starch TPS matrices to directly replace rigid, non-biodegradable petroleum polymers specifically within disposable HVAC HEPA air filter frames. This research moves beyond generic bioplastic testing to establish an application-driven baseline formulation that successfully balances adequate static structural rigidity under low-load conditions with rapid environmental decomposition after disposal, offering a clean, closed-loop material solution for the sustainable building sector.

2.0 EXPERIMENTAL PROCEDURE

2.1 Materials

Potato starch powder (purity >99%, supplied by Cap Bintang) was utilized as the primary biopolymer precursor. Analytical grade glycerol ($C_3H_8O_3$, purity >99%, Merck) was employed as the plasticizing agent. Glacial acetic acid (CH_3COOH, purity >99%, Merck) was diluted to a 10% aqueous solution and used as a chemical modifier to assist in starch destructurization. Deionized/distilled water was utilized as the solvent throughout all formulation and preparation steps. All chemical reagents were used as received without further purification.

2.2 Preparation of Modified Thermoplastic Starch

The fabrication of modified thermoplastic starch (TPS) was executed via a single-stage formulation screening based on mechanical tensile performance. The optimization was conducted by systematically varying the plasticizer (glycerol) concentration as a weight

* Corresponding to: K. C. Chong (email: chongkc@utar.edu.my)
DOI: https://doi.org/10.11113/jamst.v30n2.349

percentage (wt%) relative to the dry mass of the potato starch powder. Prior to formulation, the potato starch powder was thoroughly dried in a desiccator to eliminate residual moisture that could compromise the mechanical properties of the final polymer matrix. An aqueous solution of 10 wt% acetic acid was prepared by diluting 1 mL of glacial acetic acid with 10 mL of distilled water. This dilute acetic acid serves as a chemical modifier that assists in the destructurization of native starch granules by disrupting internal hydrogen bonds, thereby facilitating smoother hydrothermal gelatinization. The precise quantities of each constituent utilized for the initial glycerol optimization phase are detailed in Table 1.

For each formulation, 10 g of dried potato starch was weighed using an analytical balance and dispersed in 100 mL of distilled water within a glass beaker. Five discrete mass quantities of glycerol were introduced into the respective starch slurries in accordance with the experimental matrix (Table 1) to vary the plasticizer content strictly on a weight percentage (wt%) basis relative to the dry starch, followed by the addition of 1 mL of the pre-diluted 10% acetic acid solution. The constituent mixture was subsequently placed on a digital hotplate magnetic stirrer. The slurry was continuously agitated at 500 rpm and heated to a core temperature of approximately 90°C. This hydrothermal condition was maintained under constant shear for 20 mins to induce complete starch gelatinization, visually confirmed by the transition of the suspension into a homogeneous, viscous hydrogel.

The gelatinized TPS was immediately cast onto a silicone mat fitted with a structural mold frame. A precision leveling blade was employed to ensure uniform thickness and surface flatness across the cast sheet, physically controlling the deposition to yield a consistent target sheet thickness of approximately 1.0 mm ± 0.1 mm across all specimens. The cast specimens were allowed to dry via ambient evaporation at a room temperature of 25°C for 3 to 5 days. Gravimetric tracking was conducted periodically; the samples were deemed completely dry once they achieved a constant weight. The stabilized TPS sheets were then carefully demolded from the silicone substrate and prepared for destructive tensile testing to isolate the optimal glycerol-to-starch ratio demonstrating the highest ultimate tensile strength.

Table 1. Sample preparation

Sample	Weight of potato starch (g)	Weight of glycerol (g)	Glycerol to Potato Starch Dry Weight Ratio (wt.%)
C1	10.0	0.0	0
C2	10.0	2.5	25
C3	10.0	5.0	50
C4	10.0	7.5	75
C5	10.0	10.0	100

* Corresponding to: K. C. Chong (email: chongkc@utar.edu.my)
DOI: https://doi.org/10.11113/jamst.v30n2.349

2.3 Characterization and Material Testing

2.3.1 Mechanical Performance Evaluation

The mechanical properties of the TPS specimens were evaluated using a universal testing machine (INSTRON 5848 Microtester). Rectangular test specimens measuring 6 cm by 2 cm were mounted and subjected to tensile loading at a constant crosshead displacement rate of 1 mm/min until catastrophic fracture occurred. The ultimate tensile stress was continuously recorded to assess the mechanical efficacy of each additive formulation.

2.3.2 Fourier Transform Infrared (FTIR) Spectroscopy

To elucidate the chemical structural modifications and identify the functional groups within the modified TPS matrices, Fourier Transform Infrared (FTIR) spectroscopy was performed using a Nicolet iS10 spectrometer. The TPS samples formulated with varying additives were positioned directly onto the attenuated total reflection (ATR) sample holder. Spectra were acquired by scanning across a wavenumber range of 400 to 4000 cm^{-1}. The resulting absorption peaks were analyzed and benchmarked against established literature to verify the chemical interactions between the starch matrix and the additives.

2.3.3 Soil Burial Biodegradation Analysis

Biodegradation kinetics were assessed via a terrestrial soil burial assay using the optimized TPS formulation identified from the mechanical and structural characterization phases. Square specimens 1.5 cm times 1.5 cm were buried at a uniform depth of 2.5 cm within a moist soil matrix under controlled, aerobic conditions. The specimens were systematically retrieved at weekly intervals over a total duration of 6 weeks. After removal, the samples were gently cleaned of debris, dried, and weighed. The gravimetric weight loss was calculated and utilized as the primary metric to determine the quantitative biodegradation rate over time.

3.0 RESULTS AND DISCUSSION

3.1 Mechanical Performance Evaluation

To prevent premature specimen damage or localized stress concentrations at the grips caused by the compliant nature of the highly plasticized hydrogels, a low-force micro-tester (INSTRON 5848 Microtester) was selected over a high-capacity universal testing machine (e.g., Shimadzu AGS-X). This setup minimized mechanical clamp deformation on the soft polymer specimens prior to uniaxial loading.

The quantitative mechanical parameters derived from the tensile assays are compiled in Table 2. It should be noted that the values reported herein represent representative screening data utilized specifically to map the initial structural baseline trends of the biopolymer formulations. Because the mechanical drop-off between the optimal formulation (2.940 MPa) and the over-plasticized matrices (down to 0.192 MPa) spans an

* Corresponding to: K. C. Chong (email: chongkc@utar.edu.my)
DOI: https://doi.org/10.11113/jamst.v30n2.349

entire order of magnitude, the overarching structural trajectory and performance drop-off are highly conclusive. Consequently, this clear trend establishes a reliable baseline for formulation targeting without requiring extensive localized statistical variance modeling or standard deviation profiles.

As detailed in the table, the maximum tensile stress exhibited a strictly decreasing profile with increasing plasticizer concentration beyond the minimum threshold required for continuous matrix formation. For the evaluated series, the maximum recorded tensile strength was achieved at the lowest measurable plasticizer loading (Set C2, 25% glycerol), reaching an ultimate tensile stress of 2.940 MPa. Increasing the glycerol content further to 50% (Set C3), 75% (Set C4), and 100% (Set C5) led to a sharp decrement in ultimate tensile strength, falling precipitously to 0.673 MPa, 0.625 MPa, and 0.192 MPa, respectively. This inverse relationship between plasticizer loading and ultimate tensile stress highlights the dual nature of plasticization in semi-crystalline biopolymers [12].

While initial glycerol levels effectively destructurize starch granules to form a coherent film, excessive plasticizer loading heavily increases the free volume between the polysaccharide chains [13]. The surplus glycerol molecules act as molecular lubricants, decreasing intermolecular friction and reducing the cohesive energy density of the polymer network. This structural lubrication accelerates chain slippage under uniaxial tensile loading, thereby significantly reducing the maximum load-bearing capacity (ultimate tensile stress) while shifting the matrix response toward highly compliant, ductile elastomeric behavior [14]. Consequently, the minimum plasticizer concentration that balances matrix continuity with structural integrity was selected as the optimized baseline parameter for subsequent additive modifications.

To evaluate the engineering viability of the developed biopolymer, it is essential to clarify whether the obtained mechanical performance is sufficient for the intended HEPA filter frame application and benchmark it against conventional plastics and previous starch studies. Neat engineering thermoplastics traditionally specified for air filter housings, such as acrylonitrile butadiene styrene (ABS) and polypropylene (PP), exhibit high tensile strengths ranging between 30 to 45 MPa to guarantee rigid durability [15]. While the ultimate tensile strength of the optimized C2 potato-starch TPS formulation (2.940 MPa) operates an order of magnitude below these commercial petroleum-based benchmarks, it delivers sufficient structural rigidity for short-service, disposable HVAC frame configurations.

Unlike dynamic structural components, an air filter frame operates under static, uniform compressive loads within pre-existing metallic tracking channels, where the primary mechanical demand is resisting the low static pressure drop (ΔP) across the fibrous media without severe physical bowing. The 2.940 MPa mechanical threshold achieved by formulation C2 successfully meets this localized load requirement. Furthermore, compared to previous biopolymer literature, the mechanical performance of this potato-starch system stands out favorably against alternative starch sources [16]. Prior studies utilizing corn starch or cassava starch plasticized with equivalent glycerol fractions frequently report lower ultimate tensile strengths, typically hovering between 1.2 to 2.2 MPa due to smaller native granule distributions and variations in amylose-to-amylopectin ratios. The superior tensile strength realized in this study (2.940 MPa) is attributed to the larger granule architecture and unique phosphate ester group cross-linkages inherent to *Solanum tuberosum*, which optimize the cohesion of the continuous matrix post-gelatinization.

* Corresponding to: K. C. Chong (email: chongkc@utar.edu.my)
DOI: https://doi.org/10.11113/jamst.v30n2.349

Thus, while acknowledging the lower strength compared to permanent fossil-fuel synthetics, the developed formulation establishes a highly viable, eco-friendly structural baseline that successfully balances functional mechanical integrity with rapid end-of-life environmental degradation.

Table 2. Mechanical performance parameters of the fabricated TPS formulations under uniaxial tensile loading

Sample	Weight of potato starch (g)	Weight of glycerol (g)	Maximum Tensile Stress (MPa)
C1	10.0	0.0	-
C2	10.0	2.5	2.940
C3	10.0	5.0	0.673
C4	10.0	7.5	0.625
C5	10.0	10.0	0.192

3.2 Fourier Transform Infrared (FTIR) Spectroscopy

The FTIR spectra of the prepared thermoplastic starch (TPS) samples consistently display four major characteristic absorption bands, confirming the successful plasticization and retention of the biopolymer backbone (Figure 1). The broad, intense absorption band centered around 3274 cm^{-1} corresponds to O–H stretching vibrations, a profile highly indicative of robust intermolecular and intramolecular hydrogen bonding among the hydroxyl groups of both the starch matrix and the glycerol plasticizer [17].

A detailed examination of this spectral region reveals critical peak shifts and localized intensity variations that directly confirm the mechanism of hydrogen-bond formation. In its native, unplasticized state, potato starch typically exhibits a narrower O–H stretching band located at a higher wavenumber range (around 3300–3400 cm^{-1}) [18]. Upon hydrothermal processing and glycerol incorporation, the systematic migration of this band toward a lower wavenumber (~3274 cm^{-1}), accompanied by a pronounced broadening of the peak envelope, reflects a significant reduction in the vibration force constant of the hydroxyl groups [19]. This distinct shift provides definitive evidence that the highly ordered, rigid starch-starch hydrogen bonds stabilizing the native crystalline granules have been successfully disrupted and substituted by a more flexible, extensive network of starch-glycerol hydrogen bonds.

Furthermore, the systematic intensity variations observed across the different plasticizer blends correspond directly to the shifting density of these interchain linkages, validating a dynamic molecular reconfiguration within the amorphous polymer matrix. Moving lower in wavenumber, the sharp peak located near 2921 cm^{-1} is attributed to C–H stretching vibrations arising from the aliphatic hydrocarbon chains within the starch and glycerol structures [20]. A distinct, weaker absorption peak is resolved at approximately 1647 cm^{-1}, which is assigned to C=O stretching vibrations likely originating from residual acetic acid utilized during processing or bound moisture within the amorphous domains.

* Corresponding to: K. C. Chong (email: chongkc@utar.edu.my)
DOI: https://doi.org/10.11113/jamst.v30n2.349

The most prominent, sharp peak situated in the fingerprint region at 993 cm^{-1} corresponds to C–O and C–O–C stretching vibrations, which serve as a classic spectral signature of the 1,4-glycosidic bonds inherent to starch. The preservation of this peak across all modified formulations demonstrates that the primary polysaccharide backbone remains structurally intact post-processing [21]. Ultimately, the unified spectral trends confirm the successful incorporation of the biopolymer components and verify that effective matrix plasticization was achieved.

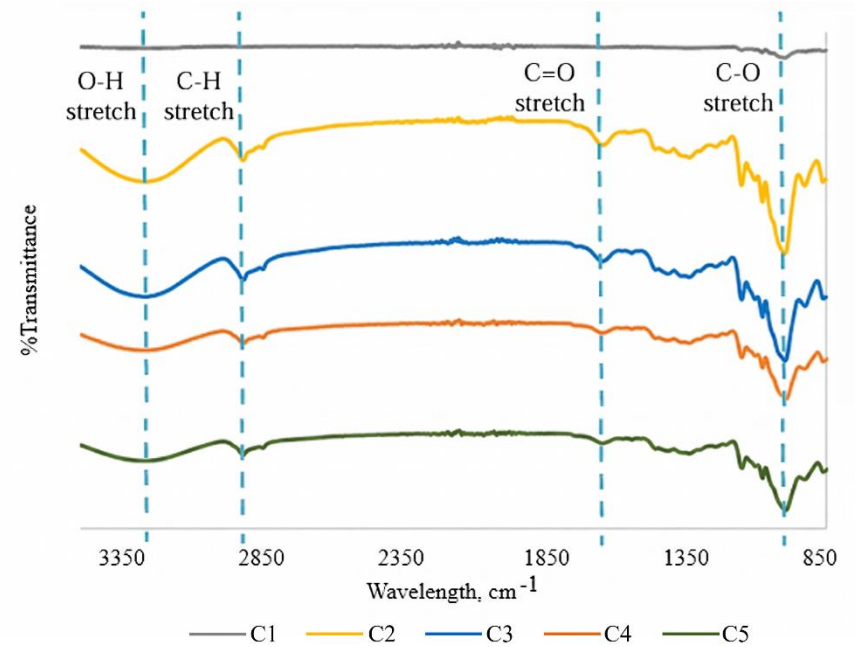

Figure 1. FTIR Spectra of the fabricated sample

3.3 Soil Burial Biodegradation Analysis

Table 3 presents the biodegradation behavior of TPS samples C1 to C5 subjected to a six-week soil burial test. The results demonstrate a significant variation in degradation performance among the formulations, with sample C2 exhibiting the highest mass loss of 79.09%, followed by C3 (72.85%), C4 (70.66%), C5 (65.63%), and C1 (23.16%). The progressive decrease in sample mass throughout the burial period indicates continuous microbial activity and hydrolytic degradation of the starch-based polymer matrices under natural soil conditions.

For all samples, a slight increase in mass was observed during the first week of burial. This phenomenon is likely attributed to moisture absorption by the hydrophilic TPS structure, particularly due to the abundance of hydroxyl groups present in starch and plasticizer components such as glycerol [22]. Water uptake promotes swelling within the polymer matrix and facilitates the penetration of microorganisms and enzymes into the material. Following this initial stage, all samples exhibited a gradual decline in mass from week 2 onwards, indicating the initiation of polymer chain scission, surface erosion, and microbial assimilation of degraded starch components [23].

Sample C1 showed the lowest biodegradation performance, with only 23.16% mass loss after six weeks. Although minor surface degradation and gradual weight reduction were

* Corresponding to: K. C. Chong (email: chongkc@utar.edu.my)
DOI: https://doi.org/10.11113/jamst.v30n2.349

observed, the sample retained much of its structural integrity throughout the test period. This behavior suggests the presence of stronger intermolecular bonding or a more compact polymer network that restricted moisture penetration and microbial accessibility [24]. Furthermore, according to structural observations detailed in environmental composting models, this slower degradation profile directly maps to a high retention of native crystallinity within the non-plasticized starch domain, which fundamentally restricts enzymatic hydrolysis [25].

In contrast, sample C2 demonstrated the highest biodegradation efficiency, where the mass decreased drastically from 0.8299 g in week 1 to 0.1555 g in week 6 (Figure 2). The rapid reduction in mass indicates extensive structural breakdown and fragmentation of the TPS matrix during soil exposure Interestingly, formulation C2 degraded more rapidly and completely than the more heavily plasticized formulations (C3–C5), revealing a distinct structural threshold in biopolymer decomposition. Consequently, the anomalous degradation rate is governed by the structural configuration of the polymer network rather than bulk thermal stability limits [26]. At a 25 wt.% plasticizer loading (C2), an optimal stoichiometric balance is achieved between the hydroxyl groups of the glycerol molecules and the active binding sites of the amylose and amylopectin chains. This balance yields a uniform, homogeneous amorphous phase that maximizes water-driven swelling and structural expansion without causing matrix collapse. This uniform swelling provides soil-born microorganisms and extracellular enzymes (such as α-amylase and glucoamylase) with unhindered, homogenous accessibility to the active α-(1,4)-glycosidic linkages.

Conversely, as the plasticizer concentration increases through formulations C3, C4, and C5 (50% to 100 wt.%), the excess glycerol far exceeds the intermolecular hydrogen-bonding capacity of the host starch network. This saturation leads to microscale phase separation, causing surplus plasticizer molecules to migrate outward and form dense, localized pools or sticky structural clusters on the material's surface [27]. These phase-separated plasticizer pools act as a highly mobile, water-soluble barrier layer that temporarily shields the underlying carbohydrate matrix. This layer interferes with genuine enzyme-substrate binding, restricts stable microbial colonization, and dilutes the concentration of localized extracellular enzymes. As a result, the surface enzymatic erosion kinetics are retarded in the over-plasticized blends, causing a progressive drop in total gravimetric mass loss as plasticizer content rises from C2 down to C5 [28].

Similar degradation trends were also observed for samples C3, C4, and C5, although at slightly lower rates. By the fifth and sixth weeks, these samples exhibited severe deterioration, suggesting advanced microbial degradation and loss of mechanical integrity. The enhanced degradation behavior of these samples may be associated with improved hydrophilicity and increased free volume within the polymer structure, which facilitated moisture diffusion and microbial colonization [29]. The differences in biodegradation performance among the TPS samples can be attributed to variations in formulation composition, starch structure, and intermolecular interactions within the polymer matrix. Samples with higher glycerol compatibility and lower crystallinity generally exhibit greater water absorption and faster degradation rates due to increased molecular mobility and accessibility to microbial enzymes [30]. Furthermore, starches with higher amylose content tend to possess a more linear molecular structure that promotes enzymatic hydrolysis, whereas highly branched amylopectin structures may hinder degradation because of their compact arrangement and higher crystalline regions [31].

* Corresponding to: K. C. Chong (email: chongkc@utar.edu.my)
DOI: https://doi.org/10.11113/jamst.v30n2.349

The biodegradation profiles obtained in this study indicate that the degradation rate of TPS materials can be tailored through formulation optimization and starch selection. Samples C2–C5 demonstrated substantial biodegradability under soil burial conditions, highlighting their suitability for environmentally friendly disposable applications and short-service-life products. In particular, the high degradation performance observed in sample C2 suggests strong potential for sustainable applications such as biodegradable packaging materials and disposable air filter frame components, where rapid environmental decomposition after disposal is desirable.

Table 3. Biodegradable test

Sample	Initial mass (g)	Mass (g)						Mass loss (%)
		Week 1	Week 2	Week 3	Week 4	Week 5	Week 6	
C1	0.7401	0.7652	0.7485	0.7152	0.6636	0.6242	0.5687	23.16
C2	0.7438	0.8299	0.7725	0.6585	0.4811	0.3460	0.1555	79.09
C3	0.7415	0.8234	0.7688	0.6631	0.5041	0.3785	0.2013	72.85
C4	0.7422	0.8125	0.7616	0.6666	0.5033	0.3624	0.2178	70.66
C5	0.7435	0.8165	0.7682	0.6788	0.5257	0.3921	0.2555	65.63

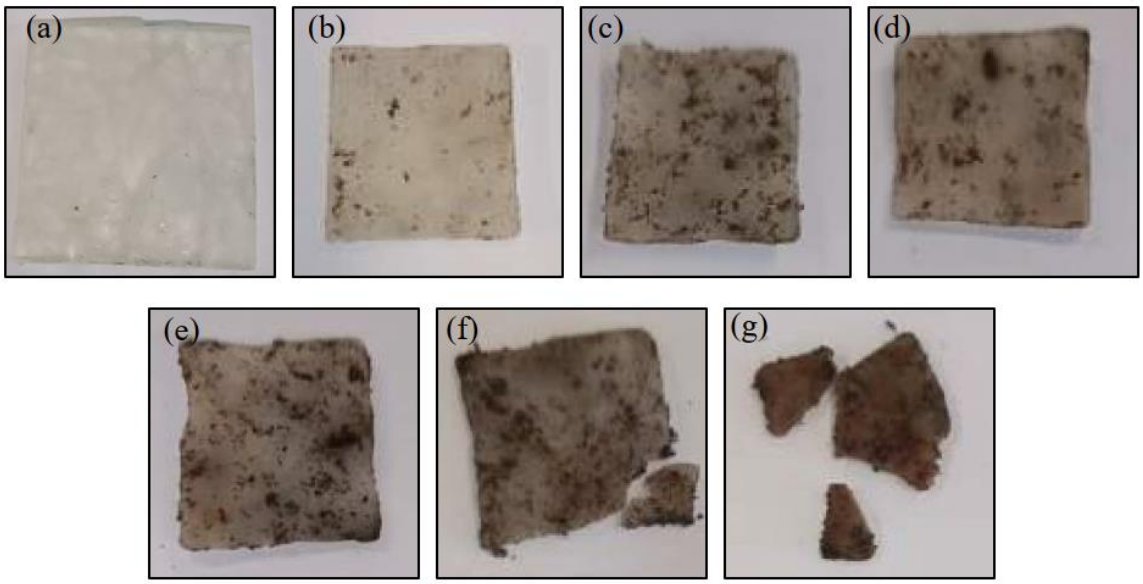

Figure 2. Sample C2 Buried in Soil at (a) Initial sample, (b) 1st week, (c) 2nd week, (d) 3rd week, (e) 4th week, (f) 5th week, and (g) 6th week

3.4 PERFORMANCE BENCHMARKING WITH PREVIOUS STUDIES

To evaluate the engineering viability and environmental efficacy of the optimized potato-starch thermoplastic starch (TPS) formulation, a comprehensive benchmarking

* Corresponding to: K. C. Chong (email: chongkc@utar.edu.my)
DOI: https://doi.org/10.11113/jamst.v30n2.349

evaluation was conducted against alternative biopolymers and conventional petroleum plastics (Table 4). The optimized potato starch matrix (C2) exhibits a significantly higher ultimate tensile strength (2.940 MPa) than alternative corn, cassava, rice, and wheat starch matrices, which typically hover below 2.2 MPa. This mechanical superiority is driven by the unique macromolecular features of *Solanum tuberosum*, which possesses exceptionally large native granules (up to 100 µm) and naturally bound, negatively charged phosphate ester groups on its branched amylopectin domains. During processing, the large granular architecture enables thorough thermal destructurization, allowing long amylose chains to leach out into a continuous, unbroken amorphous phase. Simultaneously, the electrostatic repulsion from the phosphate groups forces the chains into an extended conformation that increases cohesive energy density and creates a weak, naturally integrated ionic cross-link network that restricts chain slippage under load.

Finally, benchmarking against conventional synthetic engineering plastics like ABS and PP highlights a critical application-driven material trade-off. While fossil-fuel synthetics display vastly superior tensile boundaries (30 to 45 MPa), their recalcitrant hydrocarbon backbones persist indefinitely in landfills when permanently bonded to contaminated filter media. Conversely, the 2.940 MPa tensile threshold of the C2 formulation delivers fully sufficient structural rigidity to withstand the static compressive forces and low-magnitude airflow resistance (typical pressure drops of 150 to 500 Pa) experienced within the continuous metal tracking slots of modern air handling units. By aligning adequate static structural integrity with a clean, rapid end-of-life environmental decomposition pathway, the developed potato starch TPS formulation establishes a highly viable, ecologically responsible structural baseline for sustainable HVAC filtration frames.

Table 4. Comparative performance benchmark of the optimized potato starch TPS matrix against literature biopolymers and synthetic standards

Material Base	Plasticizer Type & Concentration	Ultimate Tensile Strength (MPa)	Biodegradation Performance (Mass Loss / Time)	Reference
Potato starch (*Solanum tuberosum*)	Glycerol (25.0 wt.%)	2.94	79.09% loss after 6 weeks	This study
Corn starch (*Zea mays*)	Glycerol (26.6 wt.%)	4.45	90% loss after 10 days	[32]
Cassava starch (*Amylum manihot*)	Polyvinyl alcohol (20.0 wt.%)	9.92	50.45% loss after 30 days	[33]
Rice bran (*Oryza sativa*)	Glycerol (33.33 wt.%)	0.88	22% loss after 24 hours	[34]
Wheat starch (*Triticum aestivum*)	Glycerol (15.0 wt.%)	4.00	80% loss after 12 days	[35]
Acrylonitrile Butadiene Styrene (ABS)*	None (Synthetic Polymer)	35 to 50	0.00% loss over 52+ weeks	[36]
Polypropylene (PP)*	None (Synthetic Polymer)	30 to 40	0.00% loss over 52+ weeks	[37]

*Common construction materials for conventional heating, ventilating and air conditioning (HVAC) filter frames

* Corresponding to: K. C. Chong (email: chongkc@utar.edu.my)
DOI: https://doi.org/10.11113/jamst.v30n2.349

4.0 CONCLUSION

Modified thermoplastic starch (TPS) films were successfully produced using potato starch and varying glycerol concentrations through a hydrothermal gelatinization process. The results demonstrated that glycerol concentration significantly influenced both the mechanical and biodegradation properties of the TPS films. Sample C2 containing 2.5 g glycerol exhibited the highest tensile strength of 2.940 MPa, indicating the optimum balance between flexibility and structural integrity. Higher glycerol concentrations reduced tensile performance due to increased polymer chain mobility and weakened intermolecular interactions. FTIR analysis confirmed the successful plasticization of the starch matrix and the preservation of the characteristic polysaccharide structure. Soil burial testing further showed that all TPS samples were biodegradable, with sample C2 exhibiting the highest mass loss of 79.09% after six weeks. The enhanced biodegradation behavior was attributed to increased hydrophilicity and microbial accessibility within the polymer matrix. Overall, the study demonstrates that the mechanical performance and degradation rate of TPS can be effectively tailored through glycerol optimization. The optimized TPS formulation shows strong potential for sustainable biodegradable applications such as disposable packaging and environmentally friendly polymer components.

DECLARATION OF GENERATIVE AI & AI-ASSISTED TECHNOLOGIES IN THE WRITING PROCESS

The authors declare that ChatGPT, an artificial intelligence language model developed by OpenAI, was used solely to improve the language, grammar, and readability of this manuscript. The authors carefully reviewed and edited the generated content and take full responsibility for the accuracy, integrity, and originality of the final manuscript.

DECLARATION OF COMPETING INTEREST

The authors declare that they have no known competing financial interests or personal relationships that could have appeared to influence the work reported in this paper.

ACKNOWLEDGEMENT

The authors would like to express their sincere appreciation to Universiti Tunku Abdul Rahman (UTAR) for the financial support provided under the UTARRF research grant scheme, Grant No. IPSR/RMC/UTARRF/2026-C1/K01. The authors also acknowledge the facilities and technical support provided throughout the completion of this study.

REFERENCES

[1] Mata, T. M., Martins, A. A., Calheiros, C. S. C., Villanueva, F., Alonso-Cuevilla, N. P., Gabriel, M. F., & Silva, G. V. (2022). Indoor air quality: A review of cleaning technologies. *ENVIRONMENTS, 9*(9), 118–146. https://doi.org/10.3390/environments9090118

[2] Tripathi, N., Misra, M., & Mohanty, A. K. (2021). Durable polylactic acid (PLA)-based sustainable engineered blends and biocomposites: Recent developments, challenges, and opportunities. *ACS ENGINEERING AU, 1*(1), 7–38.

* Corresponding to: K. C. Chong (email: chongkc@utar.edu.my)
DOI: https://doi.org/10.11113/jamst.v30n2.349

https://doi.org/10.1021/acsengineeringau.1c00011
[3] Huang, C.-H., Liu, N., Shirai, J., Cohen, M., Austin, E., & Seto, E. (2024). Effects of dust loading on the long-term performance of portable HEPA air cleaner to woodsmoke: A laboratory investigation. *INDOOR ENVIRONMENTS, 1*(4), 100057. https://doi.org/10.1016/j.indenv.2024.100057
[4] Blair, J., & Mataraarachchi, S. (2021). A review of landfills, waste and the nearly forgotten nexus with climate change. *ENVIRONMENTS, 8*(8), 73. https://doi.org/10.3390/environments8080073
[5] Popescu, C., Dissanayake, H., Mansi, E., & Stancu, A. (2024). Eco breakthroughs: Sustainable materials transforming the future of our planet. *SUSTAINABILITY, 16*(23), 10790. https://doi.org/10.3390/su162310790
[6] Taib, N.-A. A. B., Rahman, M. R., Huda, D., Kuok, K. K., Hamdan, S., Bakri, M. K. B., Julaihi, M. R. M. B., & Khan, A. (2023). A review on poly lactic acid (PLA) as a biodegradable polymer. *POLYMER BULLETIN, 80*, 1179–1213. https://doi.org/10.1007/s00289-022-04160-y
[7] Yao, X., Yang, X., Lu, Y., Qiu, Y., & Zeng, Q. (2025). Review of the synthesis and degradation mechanisms of some biodegradable polymers in natural environments. *POLYMERS, 17*(1), 66. https://doi.org/10.3390/polym17010066
[8] Nicolau, A., Mutch, A. L., & Thickett, S. C. (2024). Applications of functional polymeric eutectogels. *MACROMOLECULAR RAPID COMMUNICATIONS, 45*(24), 2400405. https://doi.org/10.1002/marc.202400405
[9] Wang, Z., Lin, Z., Mei, X., Cai, L., Lin, K.-C., Rodríguez, J. F., Ye, Z., Parraguez, X. S., Guajardo, E. M., García Luna, P. C., Zhang, J. Y. J., & Zhang, Y. S. (2025). Engineered living systems based on gelatin: Design, manufacturing, and applications. *ADVANCED MATERIALS, 37*(14), 2416260. https://doi.org/10.1002/adma.202416260
[10] Tan, S. X., Andriyana, A., Ong, H. C., Lim, S., Pang, Y. L., & Ngoh, G. C. (2022). A comprehensive review on the emerging roles of nanofillers and plasticizers towards sustainable starch-based bioplastic fabrication. *POLYMERS, 14*(4), 664. https://doi.org/10.3390/polym14040664
[11] Ding, L., Liang, W., Qu, J., Persson, S., Liu, X., Herburger, K., Kirkensgaard, J. J. K., Khakimov, B., Enemark-Rasmussen, K., Blennow, A., & Zhong, Y. (2023). Effects of natural starch-phosphate monoester content on the multi-scale structures of potato starches. *Carbohydrate Polymers, 310*, 120740. https://doi.org/10.1016/j.carbpol.2023.120740
[12] Kandil, H., & El Desouky, F. G. (2025). Plasticizer modulation of dynamic mechanical properties and dielectric performance in sodium alginate-based biopolymer films. *Journal of Inorganic and Organometallic Polymers and Materials, 35*(11), 5790–5804. https://doi.org/10.1007/s10904-025-03623-9
[13] Lin, Q., Zhou, Y., Ma, S., Lin, S., Cai, Y., Huang, Z., Miao, S., & Lu, X. (2025). New insight into the glycerol plasticizer concentration effect on the properties and microstructure of soluble *Tremella fuciformis* polysaccharide edible films. *Journal of Future Foods, 5*, 100038. https://doi.org/10.1016/j.jfutfo.2025.10.038
[14] Demiral, M. (2025). Strength in adhesion: A multi-mechanics review covering tensile, shear, fracture, fatigue, creep, and impact behavior of polymer bonding in composites. *Polymers, 17*(19), 2600. https://doi.org/10.3390/polym17192600

* Corresponding to: K. C. Chong (email: chongkc@utar.edu.my)
DOI: https://doi.org/10.11113/jamst.v30n2.349

[15] Singh, J., Kumar, R., & Chaurasiya, S. (2025). Sustainable additive manufacturing through recycled and reinforced thermoplastic composites: State of the art. *Nanoscale, 17*, 21913–21937. https://doi.org/10.1039/D5NR01975C

[16] Song, J., Ma, C., Xu, Y., Wang, Y., Wang, B., Zhang, G., Liu, X., Xu, X., Yang, Y., & Zhang, N. (2026). Mechanistic analysis of starch gelatinization properties regulated by biomolecules: A protein, non-starch polysaccharides and lipids perspective. *Critical Reviews in Food Science and Nutrition, 66*, 3434–3451. https://doi.org/10.1080/09205063.2021.2021351

[17] Garces, V., García-Quintero, A., Lerma, T. A., Palencia, M., Combatt, E. M., & Arrieta, Á. A. (2021). Characterization of cassava starch and its structural changes resulting from thermal stress by functionally enhanced derivative spectroscopy (FEDS). *Polysaccharides, 2*(4), 866–877. https://doi.org/10.3390/polysaccharides2040052

[18] Mojo-Quisani, A., Licona-Pacco, K., Choque-Quispe, D., Mamani-Condori, R., Florez-Huaracha, K., & Huamaní-Melendez, V. J. (2024). Physicochemical properties of starch of four varieties of native potatoes. *Heliyon, 10*, e35809. https://doi.org/10.1016/j.heliyon.2024.e35809

[19] Basdeki, E., Maurizzi, E., Bigi, F., Quartieri, A., Pulvirenti, A., & Tsironi, T. (2025). Functionality and storage evaluation of fish freshness indicators based on the incorporation of anthocyanins extracted from winery grape pomace into polyvinyl alcohol/starch films. *Packaging Technology and Science, 38*(10), 703–715. https://doi.org/10.1002/pts.70000

[20] Flores-Aguilar, J. F., Rivera-Guasco, R., Islas-Guerrero, G., Ibarra-Ortega, I. S., & Vázquez-Garrido, I. (2026). Fourier transform infrared spectroscopy applications for hydrotreatment catalysts: A review. *Applied Spectroscopy Reviews*, 1–40. https://doi.org/10.1080/05704928.2025.2611739

[21] Hossain, I. M., Pooja, N., Kondeti, S. S. C., Yamamoto, T., Mazumder, N., & Noothalapati, H. (2025). Direct estimation of amylose and amylopectin in single starch granules by machine learning-assisted Raman spectroscopy. *Carbohydrate Polymers, 366*, 123929. https://doi.org/10.1016/j.carbpol.2025.123929

[22] Montilla-Buitrago, C. E., Gómez-López, R. A., Solanilla-Duque, J. F., Serna-Cock, L., & Villada-Castillo, H. S. (2021). Effect of plasticizers on properties, retrogradation, and processing of extrusion-obtained thermoplastic starch: A review. *Starch – Stärke, 73*(9–10), 2100060. https://doi.org/10.1002/star.202100060

[23] Dang, K. M., & Yoksan, R. (2021). Thermoplastic starch blown films with improved mechanical and barrier properties. *International Journal of Biological Macromolecules, 188*, 290–299. https://doi.org/10.1016/j.ijbiomac.2021.08.027

[24] Wang, L., Liu, W., Chen, X., Wu, B., Bu, N., Xiao, H., Ma, C., & Hao, J. (2025). Synergistic 3D nanofibers for enhanced microbial control and moisture regulation in fruit preservation. *Chemical Engineering Journal, 501*, 160100. https://doi.org/10.1016/j.cej.2025.165047

[25] Zhang, S., Li, Y., Jiang, L., Cao, M., Xing, Z., Dong, D., & Fang, L. (2025). Insights on the characteristics of plastic surface degradation and biofilm microorganisms: Exploring the impacts of three aerobic composting (AC) as well as UV irradiation and cycles of freeze-thaw (CFTs). *Journal of Hazardous Materials, 495*, 138960. https://doi.org/10.1016/j.jhazmat.2025.138960

* Corresponding to: K. C. Chong (email: chongkc@utar.edu.my)
DOI: https://doi.org/10.11113/jamst.v30n2.349

[26] Wang, L.-C., Wang, P., Dai, Y., Yuan, B., & Zhang, L.-W. (2025). Controllable degradation of eco-friendly poly(lactic-co-glycolic acid) antifouling coatings. *Chemical Engineering Journal, 522*, 167385. https://doi.org/10.1016/j.cej.2025.167385
[27] Hao, Y., & Yang, F. (2026). Surface modification strategies for inhibiting the migration of plasticizers from plastics. *Progress in Organic Coatings, 210*, 109697. https://doi.org/10.1016/j.porgcoat.2025.109697
[28] Eelager, M. P., Masti, S. P., Dalbanjan, N. P., Madihalli, S., Gunaki, M. N., Kurbetta, L. K., Kumar, S. K. P., & Chougale, R. B. (2024). Atrazine integrated biodegradable poly(vinyl alcohol)/xanthan gum active films for mulching applications: An alternative to microplastic generation plastic mulch. *Progress in Organic Coatings, 192*, 108510. https://doi.org/10.1016/j.porgcoat.2024.108510
[29] Bueno, F., Fultz, L., Husseneder, C., Keenan, M., & Sathivel, S. (2023). Biodegradability of bacterial cellulose polymer below the soil and its effects on soil bacteria diversity. *Polymer Degradation and Stability, 217*, 110535. https://doi.org/10.1016/j.polymdegradstab.2023.110535
[30] Pustak, A., & Maršavelski, A. (2025). Enzymatic degradation of biopolymers in amorphous and molten states: Mechanisms and applications. *FEBS Open Bio, 15*(3), 412–427. https://doi.org/10.1002/2211-5463.70177
[31] Tian, Y., Wang, Y., Zhong, Y., Møller, M. S., Westh, P., Svensson, B., & Blennow, A. (2023). Interfacial catalysis during amylolytic degradation of starch granules: Current understanding and kinetic approaches. *Molecules, 28*(9), 3799. https://doi.org/10.3390/molecules28093799
[32] Abdel Hamid, E. M., Mohamed, A. E., Mohamed, A. A., Galal, A. A., Mekhemr, A. A., Saleh, E. S., Hassan, M. I., Ahmed, M. H., & Elgendy, S. K. (2025). Optimization of corn starch/glycerol, acetic acid, and cellulose fibers ratio on biodegradable plastic synthesis by Box–Behnken design (BBD). *Clean Technologies and Environmental Policy, 27*, 4433–4455. https://doi.org/10.1007/s10098-025-03135-7
[33] Ayyubi, S. N., Purbasari, A., & Kusmiyati. (2022). The effect of composition on mechanical properties of biodegradable plastic based on chitosan/cassava starch/PVA/crude glycerol: Optimization of the composition using Box–Behnken design. *Materials Today: Proceedings, 63*(Supplement 1), S78–S83. https://doi.org/10.1016/j.matpr.2022.01.294
[34] Alonso-González, M., Felix, M., & Romero, A. (2024). Development of rice bran-based bioplastics via injection molding: Influence of particle size and glycerol ratio. *Resources, Conservation & Recycling, 208*, 107713. https://doi.org/10.1016/j.resconrec.2024.107713
[35] Mohammed, A. A. B. A., Hasan, Z., Omran, A. A. B., Elfaghi, A. M., Khattak, M. A., Ilyas, R. A., & Sapuan, S. M. (2023). Effect of various plasticizers in different concentrations on physical, thermal, mechanical, and structural properties of wheat starch-based films. *Polymers, 15*(1), 63. https://doi.org/10.3390/polym15010063
[36] Maier, C., & Calafut, T. (2008). *Polypropylene: The definitive user's guide and databook*. William Andrew Publishing.
[37] Crawford, R. J., & Martin, P. J. (2020). *Plastics engineering* (4th ed.). Elsevier Science & Technology.

* Corresponding to: K. C. Chong (email: chongkc@utar.edu.my)
DOI: https://doi.org/10.11113/jamst.v30n2.349